# *In vivo* tau in epilepsy reflects clinical severity and immune- and ageing-related proteomic changes

Sang Bin Hong,[1,2,†] Yong-Won Shin,[3,†] Jangsup Moon,[2,4] Kyung-Il Park,[2,5] Ki-Young Jung,[2] Kangyoung Cho,[6] Hongyoon Choi,[7] Kon Chu[2] and Sang Kun Lee[2]

[†]**These authors contributed equally to this work.**

## Abstract

Tau pathology plays a central role in a number of neurodegenerative diseases, but its presence and relevance in epilepsy remain incompletely understood. Emerging evidence suggests that epilepsy may promote tau accumulation, yet whether this occurs *in vivo*, independent of comorbid dementia or amyloid pathology, is unclear. In this study, we combined [$^{18}$F]flortaucipir (FTP) PET imaging with high-throughput plasma proteomics to characterise regional tau deposition and its clinical and molecular correlates in non-demented epilepsy patients.

We enrolled 75 epilepsy patients and 47 age- and sex-matched healthy controls, collecting detailed clinical data, EEG features, and plasma samples for SOMAscan proteomic profiling, and plasma p-tau217, total tau, and amyloid-β measurement. A subset underwent FTP PET and [$^{18}$F]florbetaben (FBB) PET imaging. Regional standardised uptake value ratios (SUVRs) were quantified using the AAL3 brain atlas.

Compared to controls, epilepsy patients exhibited globally elevated FTP uptake across cortical regions, particularly in the lateral and medial frontal, lateral parietal, and lateral occipital brain areas, while FBB SUVRs showed nonsignificant differences. Exploratory analyses highlighted EEG slowing, multifocal discharges, and continued seizure activity during adolescence as clinical features associated with higher FTP SUVRs. In lateralised epilepsy, asymmetry indices tended to favour the hemisphere with the seizure onset zone.

Plasma proteomic analysis identified 473 differentially expressed proteins in epilepsy, enriched in pathways related to immune activation, metabolism, and cytoskeletal remodelling. Protein expression associated with regional tau SUVRs again emphasised immune pathways as well as mitochondrial dysfunction; and suggested distinct mechanisms of tau accumulation in a region-specific manner. Furthermore, using the

OrganAge algorithm, we found accelerated biological ageing in epilepsy patients across several organs, including the brain, heart, and muscle. While brain age gaps showed the strongest positive correlation with tau, the heart, pancreas, and muscle age gaps also showed correlations with regional brain tau, suggesting a link between systemic ageing and brain tau accumulation.

Together, these findings suggest that epilepsy is associated with widespread elevated tau tracer signal that relates to EEG abnormalities, clinical disease burden, and immune- and ageing-related proteomic signatures. Our results raise the possibility that tau accumulation contributes to key aspects of epilepsy pathophysiology and may have relevance for biomarker development and future therapeutic targeting.

**Author affiliations:**

1 Center for Hospital Medicine, Seoul National University Hospital, Seoul 03080, Republic of Korea

2 Department of Neurology, Seoul National University Hospital and Seoul National University College of Medicine, Seoul 03080, Republic of Korea

3 Department of Critical Care Medicine, Seoul National University Hospital, Seoul 03080, Republic of Korea

4 Department of Genomic Medicine, Seoul National University Hospital, Seoul 03080, Republic of Korea

5 Department of Neurology, Seoul National University Hospital Healthcare System Gangnam Center, Seoul 06236, Republic of Korea

6 Healthcare AI Reasearch Institute, Seoul National University Hospital, Seoul 03080, Republic of Korea

7 Department of Nuclear Medicine, Seoul National University Hospital and Seoul National University College of Medicine, Seoul, 03080, Republic of Korea

Correspondence to: Sang Kun Lee, MD, PhD

Department of Neurology

Seoul National University Hospital

101 Daehak-ro, Jongno-gu, Seoul 03080, Republic of Korea

E-mail: sangkun2923@gmail.com

Correspondence may also be addressed to: Kon Chu, MD, PhD
Department of Neurology
Seoul National University Hospital
101 Daehak-ro, Jongno-gu, Seoul 03080, Republic of Korea
E-mail: stemcell.snu@gmail.com

Hongyoon Choi, MD, PhD
Department of Nuclear Medicine
101 Daehak-ro, Jongno-gu, Seoul 03080, Republic of Korea
E-mail: chy1000@gmail.com

**Running title**: Proteome and *in vivo* tau in epilepsy

**Keywords:** neuroinflammation; neurodegeneration; biomarkers

# Introduction

Tau is a multifunctional microtubule-associated protein whose best-characterised role is the stabilization of axonal microtubules, thereby maintaining neuronal structure. Under physiological conditions, tau supports cytoskeletal integrity and axonal transport. However, in a number of neurodegenerative diseases, tau becomes abnormally hyperphosphorylated, leading to its detachment from microtubules, self-aggregation, and the formation of intracellular neurofibrillary tangles (NFTs)—a hallmark feature of Alzheimer's disease (AD) and other tauopathies. Phosphorylated tau, in particular, has been shown to correlate with disease severity, cognitive decline, and clinical progression in AD and related conditions.[1–3]

Recent evidence has pointed to a possible role for tau pathology in epilepsy, a chronic neurological disorder characterised by hyperexcitable neuronal circuits and recurrent

seizures. In vivo animal studies have demonstrated that increased neuronal activity elevates extracellular tau levels,[4] while tau overexpression or mutation can trigger seizures in experimental models.[5,6] Conversely, genetic or pharmacologic reduction of tau has been shown to attenuate seizure severity and reduce mortality.[7–9] Postmortem studies and analyses of surgically resected human brain tissue from epilepsy patients have revealed elevated phosphorylated tau levels, particularly in cases of temporal lobe epilepsy and epilepsies associated with inflammation or brain injury.[10–13]

Despite these findings, it remains unclear whether pathologic tau accumulation occurs *in vivo* in epilepsy patients without comorbid dementia, and whether such accumulation is linked to clinical features such as epilepsy duration, seizure frequency, or electrophysiological abnormalities.

The development of PET tracers targeting phosphorylated tau has enabled noninvasive visualisation of tau pathology in humans. [$^{18}$F]Flortaucipir (AV-1451, FTP) is a widely used PET ligand that binds with relative specificity to paired helical filaments and neurofibrillary tangles, exhibiting strong specificity for tau aggregates in AD.[14,15] The present study aimed to characterise *in vivo* tau deposition in nonlesional epilepsy patients using FTP PET imaging and to examine its relationship with clinical measures of epilepsy severity, including seizure burden and electrophysiological abnormalities.

While PET imaging offers a valuable snapshot of regional tau accumulation, it provides limited insight into the molecular mechanisms driving tau pathology in epilepsy. To address this gap, we integrated PET imaging with aptamer-based high-throughput proteomic profiling (SOMAscan)[16] to identify co-regulated proteins and pathways associated with elevated tau deposition. Prior studies have identified shared proteomic signatures between epilepsy and AD,[17] and proteomic analyses in epilepsy have identified proteins either interacting with tau directly or regulated by tau expression.[18] We conducted a comprehensive molecular analysis to uncover potential mechanisms linking systemic proteomic changes to tau deposition.

By integrating these imaging and proteomic approaches, we aimed to assess the extent of brain tau deposition in epilepsy, to provide insight into its underlying mechanisms, and to suggest potential therapeutic strategies targeting tau-related processes in epilepsy.

# Materials and methods

## Participants and general outline

We recruited ambulatory epilepsy patients who visited the Seoul National University Hospital epilepsy clinic from 2021 to 2024, with no reported memory complaints, without other diagnoses of neurodegenerative diseases including Parkinson's disease, multiple system atrophy, amyotrophic lateral sclerosis, and all types of dementia or a Mini-Mental State Examination (MMSE) score below 25, and without a history of major or repetitive head trauma. Epilepsy patients meeting inclusion criteria were recruited from the pool of patients admitted to the epilepsy monitoring unit (EMU) for 24-hour video-EEG monitoring (VEM) for clinical reasons, such as to optimize anti-seizure medication use, to observe seizure semiology and document EEG changes, and to differentiate nonepileptic events from true seizures. During the admission, we obtained morning blood plasma samples (before 10AM) for quantification of phosphorylated tau 217 (p-tau217), amyloid-$\beta_{40}$, amyloid-$\beta_{42}$, and SOMAscan proteomic profiling for all patients with written agreement to participate in the study. These patients additionally underwent routine ApoE genotyping, and completed the MMSE, the Patient Health Questionnaire-9 (PHQ-9), and the Pittsburgh Sleep Quality Index (PSQI) questionnaire, all as part of the research protocol. Patients without brain MRIs taken in the past year were scheduled to complete 3.0 tesla brain MRI scans within three months of the EMU admission as part of the clinical work up.

A subset of patients without structural abnormalities on MRI was selected for FTP PET imaging. Structural normality was defined by the absence of: (1) space-occupying lesions, including tumours or vascular malformations; (2) focal encephalomalacia or other acquired lesions attributable to prior stroke or haemorrhage; and (3) hydrocephalus. We did not classify hippocampal sclerosis as a structural abnormality, as it reflects a degenerative process intrinsically associated with epileptogenesis and exists along a spectrum of severity, rather than representing a discrete focal abnormality that would confound PET image interpretation. In addition, epilepsy patients willing to undergo an additional scan were evaluated with [$^{18}$F]florbetaben PET (FBB) scans to assess amyloid burden.

Age- and sex-matched control participants without history of epilepsy, evident brain lesions, and cognitive complaints also underwent SOMAscan, p-tau217, and amyloid-$\beta_{40/42}$ measurements, the MMSE, and completed the PHQ-9 and PSQI questionnaires. Similar to the epilepsy cohort, a

subset of these controls additionally underwent FTP PET and FBB PET imaging. Detailed methods for plasma proteomic profiling, p-tau 217, total tau, amyloid-$\beta_{42}$ and amyloid-$\beta_{40}$ measurements are provided in the **Supplementary Methods**. The study was approved by the Institutional Review Board of Seoul National University Hospital (IRB No. 2102-046-1196), and written informed consent was obtained for all participants.

## Clinical assessment

For all epilepsy patients, we collected detailed clinical data, including epilepsy duration, seizure type and epilepsy etiology, anti-seizure medication (ASM) use, and baseline monthly seizure frequency. Epilepsy duration was defined as the time elapsed since first diagnosis (in months). Additional information was collected regarding seizure persistence during childhood (1–10 years) and adolescence (11–18 years). Data on medical comorbidities and years of education were also recorded. Each patient was categorised as one of the following: (i) Generalised epilepsy – generalised epileptiform discharges on EEG with congruent clinical features (e.g. juvenile myoclonic epilepsy); (ii) Epilepsy with hippocampal sclerosis (HS): definite HS on MRI with a seizure onset zone ipsilateral to the pathological side; (iii) Nonlesional epilepsy – focal-onset recurrent seizures without an identifiable structural lesion on MRI; (iv) Postencephalitic epilepsy – recurrent seizures following CNS infection, autoimmune encephalitis, or new-onset refractory status epilepticus; or (v) Lesional epilepsy – epilepsy attributable to an MRI-detectable structural lesion.

In addition, 24-hour video-EEG recordings were analysed to assess for abnormalities The predominant frequency of the posterior dominant rhythm during wakefulness was quantified as a measure of background activity. Spike frequency was classified according to the American Clinical Neurophysiology Society's standardised critical care EEG terminology.[20] The presence of focal or generalised slowing was recorded. Interictal epileptiform discharges were categorised by frequency as abundant (>1 per 10 s), frequent (≥1 per min but <1 per 10 s), occasional (≥1 per h but <1 per min), or rare (<1 per h). Spatial distributions of interictal discharges were classified as focal or multifocal. Epilepsy laterality was determined from the VEM data, and patients were subsequently categorised as having generalised, left-, right-, bilateral-, or indeterminate-lateralised epilepsy.

## PET imaging

Detailed acquisition parameters for FTP and FBB PET are provided in the **Supplementary Methods**.

Region-based standardised uptake value ratio (SUVR) values were extracted using the Automated Anatomical Labelling (AAL3) atlas in MNI space. Quantification of PET images were performed using the BTXBrain software (Brightonix Imaging, Seoul, Korea). In brief, spatial normalisation of PET images was conducted onto the MNI standard space using a deep learning-based algorithm incorporated in the software.[20] Regional uptake values were extracted based on the AAL3 atlas, which was predefined in the normalised space. SUVRs were calculated by dividing the mean uptake values in each target region by the mean uptake in the cerebellar grey matter, which served as the reference region. For each participant, mean SUVR values were calculated for each ROI.

For FBB PET, amyloid imaging was additionally interpreted visually by experienced nuclear medicine physicians as part of routine clinical practice. Visual assessments were independently performed by more than two readers. Amyloid plaque burden was qualitatively evaluated using the Brain Amyloid Plaque Load (BAPL) scoring system, where BAPL scores of 1, 2, and 3 indicate no, minor, and significant amyloid deposition, respectively. The interpretation followed the standardised guidelines for FBB PET imaging.[21]

## Regional SUVR comparisons across groups and subgroups

To examine and display spatial patterns of FTP uptake in a more intuitive way, SUVRs from AAL3 cortical subregions were aggregated into 12 brain regions representing medial, lateral, and ventral cortical areas: lateral frontal, medial frontal, ventral frontal, sensorimotor, posterior cingulate–precuneus, insula, lateral parietal, lateral temporal, medial temporal, lateral occipital, medial occipital, and fusiform cortex. All subsequent analyses were conducted using these 12 composite regions to ensure consistency across comparisons.

Group differences in regional SUVRs between epilepsy patients and controls were assessed using linear regression, adjusting for age, sex, and education, and associated unadjusted and adjusted *p*-values were derived for each region. Additional analyses to test for the dissociation between FTP and FBB uptake values as well as comparing inter-individual variability in FTP signal between epilepsy and controls are supplied in the **Supplementary Methods**.

Associations between regional tau SUVRs and clinical or EEG variables were examined using an exploratory two-stage approach. Initial screening of associations was performed using partial correlation analyses adjusted for age and sex for continuous variables, and covariate-adjusted linear models for categorical variables. Standardised effect sizes were derived from model statistics for visualisation.

To formally evaluate statistical significance while accounting for repeated regional and hemispheric measurements within individuals, linear mixed-effects models were fitted with regional SUVR as the dependent variable, clinical or EEG variables as fixed effects, age and sex as covariates, and subject as a random intercept. Standardised coefficients were used to summarise effect sizes. For categorical predictors, similar mixed-effects models were fitted with group as a fixed effect and subject as a random intercept. Where nominal evidence of association was observed (unadjusted $p$-value < 0.05), post hoc pairwise comparisons were performed using estimated marginal means with Tukey correction. Post hoc analyses were conducted separately within each brain region and hemisphere.

False discovery rate (FDR) correction was applied to account for multiple testing across regions and hemispheres, where indicated. All analyses were considered exploratory and hypothesis-generating.

## Asymmetricity of [$^{18}$F]flortaucipir and [$^{18}$F]florbetaben uptake

Asymmetry indices were calculated to assess hemispheric differences in FTP and FBB SUVRs. The asymmetry index was defined as:

$$Asymmetry\ index\ (AI) = \frac{L - R}{L + R}$$

Where $L$ is the SUVR of the left brain region, and $R$ is the SUVR of the right brain region. Positive values indicate leftward asymmetry and negative values indicate rightward asymmetry of tracer uptake.

## MRI acquisition and regional volume *Z* score derivation for epilepsy patients

Detailed methods to derive regional cortical volume Z-scores from structural MRI using a normative reference sample are presented in the **Supplementary Methods**.

## Differential protein expression analysis

Individual aptamers were mapped to nonduplicated EntrezGeneSymbols and raw values were log transformed for downstream analysis. Differential expression of proteins was analysed with the limma package in R, adjusting for age and sex. Proteins with an adjusted *P*-value (Benjamini-Hochberg) < 0.05 and |log2 fold-change| > 0.5 were considered differentially expressed. Significantly over- and under-expressed proteins were then annotated with gProfiler.

Partial correlation coefficients adjusting for age and sex were calculated between protein expression levels and regional tau tracer signal across brain regions in epilepsy patients and controls. We visually examined the correlation patterns of top 50 positively and negatively correlated proteins across brain regions in a hierarchically clustered heatmap. Proteins showing nominally significant correlations with tau in at least one brain region were retained for further analysis ($M_{eff}$ adjusted *P*-values < 0.1). Proteins significantly positively and negatively correlated with regional brain tau were subjected to pathway enrichment analysis using gProfiler. Significantly enriched biological processes and signalling pathways were identified based on Gene Ontology (GO), and KEGG/Reactome annotations (adjusted *p*-value < 0.05).

We also used the OrganAge[22] algorithm to estimate organ-specific biological age gaps based on each subject's proteomic profile. OrganAge gaps were calculated as the difference between predicted organ age and chronological age relative to the reference population based on models developed by Oh et al.[22] Organ age *Z* scores were the standardised organ age gaps based on model variability per organ to allow for comparisons across organs. Positive, higher *Z*-scores indicate accelerated organ ageing, whereas negative, lower *Z*-scores reflect preserved or decelerated ageing We compared organ age gaps between epilepsy patients and controls and evaluated the association between organ age gaps (across 11 organs and overall systemic ageing as measured by the organismal age gap) and regional tau SUVRs across 12 brain regions in epilepsy patients, with partial correlations adjusting for age, sex, and comorbidities. We further conducted correlation analysis between organ age gap and clinical factors.

## Statistical analysis

All statistical analyses were performed using R (v4.4.1) and Python (v3.12.4), with a significance threshold set at two-sided *p*-value < 0.05, unless otherwise specified. Variables exhibiting non-normal distribution were either log-transformed (in case of raw RFU values) or analysed using non-parametric methods. Baseline demographic and clinical characteristics were

compared using independent samples t-tests or Wilcoxon rank-sum tests for continuous variables, and Chi-square tests or Fisher's exact tests for categorical variables. To assess associations between FTP SUVRs and clinical variables, we used multivariable linear regression models adjusted for age and sex, as well as age, sex, and years of education. To assess correlations between FTP SUVRs in brain regions and protein expression and organ age gap *Z*-scores, we used partial correlations adjusting for age, sex, and comorbidities using the *ppcor* package in R.

For the differential protein expression analysis, FDR < 0.05 and absolute $\log_2$ fold change ≥ 0.5 were considered statistically significant. For calculating adjusted *P*-values in correlations between nonindependent variables, such as nearby brain areas, we used the Li and Ji method to calculate the number of effective comparisons ($M_{eff}$).

Plots were generated using *nibabel*, *ggplot2*, *ComplexHeatmap*, and *EnhancedVolcano*.

# Results

Of 168 patients approached, 75 epilepsy patients and 47 healthy volunteers were included in the study. (**Table 1, Supplementary Figure 1**). Plasma proteomic profiles (SOMAscan) were assessed in 73 epilepsy patients and 43 controls. Morning plasma for p-tau217, total tau, and amyloid-$\beta_{42/40}$ ratios were obtained in 39 epilepsy patients and 37 controls. ApoE genotyping was successfully performed in 40 epilepsy patients and 25 controls. ApoE genotyping was not available for all participants, primarily due to refusal to consent to genetic testing. There was no systematic difference in demographic or clinical characteristics between participants with and without available ApoE genotype data. 57 lesion-negative epilepsy patients were eligible for FTP PET imaging, of whom 32 completed tau PET. Twenty-four controls underwent tau PET. A subset (20 epilepsy patients and 7 controls) of the participants who underwent tau imaging also completed FBB PET scans.

The epilepsy cohort was slightly younger and had a lower prevalence of hypertension than the control group, but there were no significant differences in years of education, other comorbidities, sex distribution, APOE allele frequency, MMSE scores, sleep quality (PSQI), or

depression scores (PHQ-9). Demographic and clinical characteristics are presented in **Table 1** and **Supplementary Table 1**. Among postencephalitic epilepsy patients, two had a suspected autoimmune cause, and three had a history of new onset refractory status epilepticus after a febrile prodrome. History of status epilepticus was present in eight of 75 patients.

Plasma levels of total tau and the amyloid-$\beta_{42/40}$ ratio did not significantly differ between groups. Although mean p-tau 217 levels were not significantly elevated in epilepsy patients (Epilepsy - Control β: 0.15, 95% CI [-0.04,0.34], *p*-value = 0.12), significantly more epilepsy patients had p-tau 217 levels exceeding the upper normal limit of 0.42 (24% vs 5%, Fisher's exact test *P*-value 0.03).[23] Plasma p-tau217 levels and amyloid-$\beta_{42/40}$ ratios were not significantly correlated with regional tau SUVRs, although modest positive trends were observed in a subset of regions (**Supplementary Figure 2**). Among participants who underwent FBB PET, the proportion of amyloid-negative scans was comparable between groups: 90.0% in epilepsy patients and 86.7% in controls.

## Comparison of regional [$^{18}$F]flortaucipir and [$^{18}$F]florbetaben SUVR values between epilepsy and controls

Patients with epilepsy demonstrated significantly higher FTP uptake across nearly all cortical regions compared to controls (**Figure 1A; Supplementary Table 2, Supplementary Figure 3**), and this tendency was more pronounced in the right hemisphere than the left (**Supplementary Figure 3 & 4**).

Although differences in FTP SUVR were broadly distributed across the cortex, they were most prominent in the frontal areas, where controls had very low levels of SUVR. Medial and ventral brain regions (medial temporal, the fusiform gyrus, orbitofrontal cortex and the inferior occipital lobe) demonstrated higher SUVRs than the frontal regions in both epilepsy and controls, and the gap between epilepsy and controls was less prominent in these regions (**Figure 1B, Supplementary Figure 3 & 4**). The differences in SUVRs between epilepsy and controls remained statistically significant in most brain areas in linear models correcting for years of education in addition to age and sex (**Supplementary Table 3**), as well as when late-onset epilepsy patients (epilepsy onset after age 60, N=12) were excluded (**Supplementary Table 4**). Visualisation of age- and sex- adjusted effect sizes of epilepsy status on regional FTP SUVRs

emphasised the left medial and lateral temporal areas and right frontal and mid-cingulate areas (**Supplementary Figure 6**).

In contrast, FBB uptake in epilepsy patients was not statistically different from controls. Analysis of age- and sex-adjusted average effect sizes revealed positive values across a broad range of brain regions (**Supplementary Table 5**), but none of the effect sizes were statistically significant.

Although higher FTP uptake was seen across the majority of brain areas in epilepsy, there was a significantly increased inter-individual variability of regional FTP SUVRs in epilepsy compared to controls (**Supplementary Figure 7A-B**). Moreover, the FTP SUVRs were elevated beyond what could be expected from FBB SUVR compared to controls (**Supplementary Figure 7C-D**).

## Clinical factors associated with regional [$^{18}$F]flortaucipir SUVR

We next examined whether regional tau tracer uptake was associated with clinical features reflecting epilepsy severity. Exploratory partial correlation analyses hinted at an association between regional SUVRs and EEG slowing, presence of multifocal discharges, as well as the presence of continued seizures during adolescence (**Figure 1C-D**).

Linear mixed-effects models accounting for repeated regional and hemispheric measurements within subjects identified several clinical and EEG markers of epileptogenicity associated with regional tau tracer SUVRs (**Supplementary Table 6)**. The presence of multifocal discharges showed the strongest association with FTP SUVRs ($\beta = 0.051$, SE = 0.016, unadjusted $p$-value = 0.003), remaining significant after FDR correction ($P_{FDR} = 0.035$). EEG slowing ($\beta = 0.042$, SE = 0.017, unadjusted $p$-value = 0.019) and a history of adolescent-onset seizures ($\beta = 0.047$, SE = 0.019, unadjusted $p$-value = 0.022) were also associated with higher FTP SUVRs at the nominal level, although these associations did not survive FDR correction. Uncontrolled epilepsy showed a weaker and non-significant trend toward higher FTP uptake ($\beta = 0.034$, $p$-value = 0.098) and spike frequency ($Z$-scored) was not significantly associated with regional FTP SUVRs ($\beta = 0.012$, $p$-value = 0.171).

Post hoc analyses of multifocal discharges, EEG slowing, and seizures during adolescence revealed that multifocal discharges were associated with widespread and FDR-significant increases in regional FTP uptake, and whereas EEG slowing and adolescent-onset seizures

showed weaker, regionally variable effects that did not survive correction for multiple comparisons except for EEG slowing and the medial occipital cortex (**Figure 2, Supplementary Table 7**). Further visualisation of the FTP SUVR distributions for individual clinical factors is provided in **Supplementary Figures 8-12**.

We also compared the distribution of FTP SUVRs depending on ApoE4 carrier status, which appeared to have no significant effect on tau SUVRs, as ApoE4 carriers and non-carriers had similar levels of FTP uptake across brain areas (**Supplementary Figure 13**).

## Regional [$^{18}$F]flortaucipir SUVRs show differences in epilepsy subtypes

Amongst different epilepsy etiologies, postencephalitic epilepsy tended to have the highest average FTP uptake in most brain regions, including the medial frontal, and medial occipital regions (**Figure 3A**). Generalised epilepsy and epilepsy with hippocampal sclerosis generally had lower FTP SUVRs than the other two etiologies, with the exception of hippocampal sclerosis in the medial temporal area, where average FTP SUVR was greatest in epilepsy with hippocampal sclerosis (**Figure 3A**). This observation remained unchanged even with analysis after removing the hippocampus proper from the medial temporal region of interest (**Supplementary Figure 14**).

## Asymmetricity of regional [$^{18}$F]flortaucipir SUVR and [$^{18}$F]florbetaben SUVR

We next examined the laterality of tracer uptake for both FTP and FBB. In both epilepsy and controls, there was a uniform tendency for greater average FTP tracer uptake in the right hemisphere for the fusiform gyrus and lateral temporal, medial temporal, and medial frontal regions, whereas greater left average tau tracer uptake was seen in the insula. Average FBB tracer uptake was greater in medial frontal, sensorimotor, insula, lateral temporal, and medial occipital regions.

We also wanted to examine whether FTP SUVRs exhibited hemispheric asymmetry in patients with lateralised seizure onset zones. In patients whose seizures originated in the left hemisphere, we observed greater mean asymmetry indices – i.e. greater left-ward bias in FTP tracer uptake – than in patients with right-sided epilepsy in 9 out of 12 brain regions, indicating a tendency for more tau tracer uptake ipsilateral to the seizure onset zone (**Figure 3B**). Baseline FTP uptake

asymmetry derived from controls (green line in **Figure 3B**) often was located in between the mean asymmetry index of left and right lateralised epilepsy patients, indicating asymmetry congruent with the seizure onset hemisphere exists on top of baseline asymmetry. The difference in mean asymmetry index was more pronounced in the lateral than medial cortical regions, including the lateral occipital and lateral parietal lobes. Individual profiles of asymmetry indices for left and right lateralised patients as well as corresponding atrophy maps are provided in **Supplementary Figures 16-17**.

We saw a similar pattern for lateralised epilepsy in FBB SUVRs, with 9 out of 12 brain regions having a higher average uptake in the epileptogenic hemisphere (**Supplementary Figure 15**).

## Individual patterns [$^{18}$F]flortaucipir uptake and brain atrophy in epilepsy

Visual assessment of regional tau tracer uptake and cortical volume revealed no consistent spatial correspondence at the group level (**Supplementary Figure 6**). Correlation between individual regional FTP SUVRs and MRI-derived cortical volumes showed no significant trends, with partial correlation coefficient $r_p$ ranging from -0.44 to 0.49 and all $P_{FDR} > 0.64$ (**Supplementary Table 8**).

Individual-level inspection demonstrated marked heterogeneity in the relationship between tau deposition and atrophy. Patients generally had a region with focally elevated FTP uptake in the hemisphere with the seizure onset zone (**Figure 4A-B**). A patient with right hippocampal sclerosis showed focal right hippocampal atrophy with relative preservation of other regions, alongside elevated FTP uptake in the bilateral temporal poles and inferior temporal cortices (**Figure 4C**). One patient with postencephalitic epilepsy showed bilateral hippocampal atrophy, but increased FTP uptake in the left parieto-occipital cortex, as well as the right cingulate cortex (**Figure 4D**).

Notably, one patient with a short history of mild seizures nonetheless exhibited widespread FTP uptake and cortical atrophy (**Figure 4E**) and was subsequently diagnosed with AD at 3 years of follow-up. This pattern of intense hippocampal uptake extending into the parahippocampal gyrus was not observed in other epilepsy patients, suggesting a distribution distinct from that seen in other patients. Further examples of individual cases are provided in **Supplementary Figures 16-18**.

## Differentially expressed proteins in epilepsy

To explore potential molecular pathways contributing to increased tau tracer signal in epilepsy, we next analysed differentially expressed plasma proteins between epilepsy patients and controls. A total of 473 proteins were significantly altered in epilepsy, with 462 upregulated and 11 downregulated compared to controls (**Figure 5A, Supplementary Table 9**). Pathway enrichment analysis of the upregulated proteins revealed significant involvement of endocytosis, the ErbB signalling pathway, and components of both the innate and adaptive immune systems (**Figure 5B**).

Among individual proteins in the set of differentially expressed proteins, a large number of eukaryotic translation initiation factors were the most highly overexpressed, including EIF4A1 ($log_2$FC 0.97, $P_{FDR}$ 1.55e-6) and EIF4A2 ($log_2$FC 0.78, $P_{FDR}$ 4.08e-6), the latter of which has been implicated in developmental epileptic encephalopathy.[24] Multiple RNA-binding proteins, particularly members of the hnRNP family (e.g., HNRNPK, HNRNPF, HNRNPA1, HNRNPAB), were also upregulated. hnRNPs have been implicated in neurodevelopmental disorders and their importance in controlling synaptic plasticity and axonal function are increasingly recognised.[25,26] Plasma of epilepsy patients also had an increased abundance of ubiquitin- and SUMO-conjugating enzymes, including UBE2I, UBE2D4, UBE2K, and UBE2V1/2, indicating disruption of the ubiquitin-proteasome system (UPS), consistent with a few prior studies that have implicated the UPS in epilepsy.[27-29]

Several of the prominently downregulated proteins included mitochondrial assembly and respiratory-chain components including NDUFAF1 ($log_2$FC -0.84, $P_{FDR}$ 0.02) and MRPL14 ($log_2$Fc -0.51, $P_{FDR}$ 0.04) and respiratory-chain regulator COX7A2L ($log_2$Fc -0.73, $P_{FDR}$ 0.04), aligning with previous findings of impaired oxidative phosphorylation and mitochondrial ribosomal function in epilepsy.[30–32] Cytoskeletal and contractile proteins such as ACTN2, MYBPC1, and MYOM2 were also decreased.

## Proteins associated with regional [$^{18}$F]flortaucipir SUVRs in epilepsy patients imply diverse mechanisms of tau accumulation

An exploratory correlation analysis between protein expression and tau SUVR across all brain regions in epilepsy patients identified 70 proteins positively and 54 negatively correlated with regional brain tau at a nominal $M_{eff}$-adjusted $p$-value < 0.1. In controls, 26 proteins were positively correlated and 155 negatively correlated with brain tau at $M_{eff}$-adjusted $p$-value < 0.1, with minimal overlap between the correlated protein sets of epilepsy and controls.

Pathway enrichment analysis revealed that, in epilepsy, proteins showing nominal positive correlation with regional tau signal were substantially enriched for mitochondrial functions—including acetyl-CoA biosynthetic processes and mitochondrial compartments—as well as cellular stress response, cytokine activity, and ErbB signalling pathways (**Figure 6A**). In contrast, proteins showing predominantly negative correlations with regional tau signal were enriched in innate immune pathways such as IL-17 signalling, Toll-like receptor signalling, granulocyte chemotaxis, leukocyte aggregation, and in adaptive immune pathways including B cell receptor and T cell modulation pathways (**Figure 6B**). While proteins negatively correlated with tau in controls were also enriched in immune-related pathways (**Supplementary Figure 19**), there was distinct lack of overlap between epilepsy-associated proteins and regional tau-associated proteins in epilepsy, suggesting unique mechanisms underlying tau aggregation in epilepsy.

The proteins related to mitochondrial function that showed nominal positive correlations with regional tau signal were mitochondrial and metabolic enzymes including CBR4, ACAA1, DLAT, PDHX, FDPS, and COQ6, and regulators of oxidative stress including NFE2L2, GSTA1, ULK3, and ALKBH2, aligning with previous reports of tau-associated alterations in oxidative metabolism and mitochondrial dynamics.[33,34] The immune-associated proteins with nominal negative associations with regional tau signal included several of the S100 proteins that are markers of activated microglia including S100A8, S100A9, and S100A12, as well as chemokines that recruit immune cells such as CCL7 and CCL15. Concurrently, increased abundance of inhibitory immune receptors such as LILRA2A and LILRB3, and immunomodulatory enzyme IL4I1 were also nominally associated with decreasing regional FTP uptake.

We next visualised the regional correlation patterns for the top 50 positively and negatively correlated proteins in epilepsy and controls (**Supplementary Figures 20-21**). The associations were distributed unevenly across brain regions in epilepsy. In particular, the fusiform gyrus, which exhibited the greatest number of positively correlated proteins in both epilepsy and controls, and the medial temporal cortex had a correlation pattern distinct from that of parieto-occipital areas in epilepsy. In controls, the distribution of correlations among top negatively correlated proteins was more uniform across most brain regions. This may indicate a stronger region-specific mechanism for tau accumulation in epilepsy, different from the pattern observed in controls.

## Accelerated organ ageing in epilepsy and its relationship with regional [$^{18}$F]flortaucipir SUVR

In the subsequent analysis, we used the OrganAge[22] algorithm to estimate predicted organ age from proteomic data and calculated the organ age gap for each subject and organ. Epilepsy patients exhibited significantly greater age gaps than controls in the brain, kidney, muscle, pancreas, and in overall organismal age (**Figure 7, Supplementary Figure 22, Supplementary Table 10**). This trend was preserved after adjusting for comorbidities and lifestyle differences including hypertension, type 2 diabetes mellitus, heart disease, kidney disease, smoking, and alcohol consumption (**Supplementary Table 10**).

Correlation analyses between organ age gap and regional FTP SUVR revealed notable differences between epilepsy patients and controls (**Supplementary Figure 23, Supplementary Table 11**). Overall, correlations were more negative in the epilepsy group. In particular, immune age gap was not positively correlated with tau signal in epilepsy, whereas a strong positive correlation was observed in controls. There was a significant negative association between organ age gap Z-scores and chronological age (Pearson's correlation coefficient = –0.23, 95% CI [-0.28,-0.19], $p$-value < 2.2e-16), which may have contributed to the overall negative correlation values seen in epilepsy.

Despite this general pattern, both brain and heart organ age gaps exhibited predominantly positive correlations with tau signal across most brain regions, with the strongest associations observed in the medial occipital and lateral parietal cortices. The muscle organ age gap showed the strongest correlation with FTP signal in the sensorimotor area, highlighting a potential

connection between peripheral and central ageing processes in epilepsy (**Supplementary Figure 23**).

Several clinical features including number of ASMs and epilepsy duration correlated strongly with organ age gap, suggesting that at least a few epilepsy-related factors are linked to organ ageing (**Supplementary Figure 24)**.

# Discussion

This is the first study to our knowledge to observe consistently increased brain FTP uptake *in vivo* in a substantial number of non-demented epilepsy patients with a range of clinical severities. Increased FTP SUVRs compared to controls was most pronounced in the frontal and lateral cortical regions and correlated with markers of epilepsy severity, and especially with EEG markers of diffuse epileptogenicity. Lateral cortical FTP signal tended to display hemispheric asymmetry consistent with seizure lateralization, whereas regional brain atrophy did not seem to correlate with FTP SUVRs. Exploration of differentially expressed proteins in epilepsy highlighted altered mRNA processing, proteostasis, immune system, and mitochondrial metabolism, among other pathways. Protein expression nominally associated with regional FTP signal emphasised the involvement of metabolic, oxidative-stress, cytoskeletal, and immune pathways. Accelerated systemic and organ ageing was observed in epilepsy, with brain, heart, and muscle age gaps correlating with tau tracer uptake in the parieto-occipital brain regions.

Few prior studies have examined neurodegenerative pathology in vivo in epilepsy. Lam *et al.*[35] reported asymmetric tau and amyloid deposition co-localising with epileptogenic hemispheres in Alzheimer's disease patients with comorbid epilepsy, while Joutsa *et al.*[36] demonstrated accelerated amyloid accumulation with frontal predominance in childhood-onset epilepsy. Our findings add to this limited body of work by demonstrating increased FTP signal in non-demented epilepsy patients, with a regional distribution broadly overlapping these prior observations.

Although FTP uptake in epilepsy patients was significantly higher than in controls, it is important to note that FTP SUVRs did not reach the levels typically observed in advanced AD,[37]

where FTP retention is most intense in temporal and parietal association cortices.[38] In AD, FTP retention reaches markedly higher values and follows a pattern of spread beginning in the medial temporal lobe and expanding toward higher association cortices, and reaching the primary cortices in the late stage. With this hierarchical pattern of tau spread, the primary somatosensory and motor cortex would be the least affected by tau, whereas in epilepsy, no such pattern was seen. This suggests that if tau pathology is present and clinically relevant in epilepsy, its magnitude and distribution could result from a mechanism distinct from that of AD, possibly related to chronic seizures and inflammation.[39,40] Although FTP signal observed in our study are unlikely to represent classic AD-type neurofibrillary tangles, previous studies confirm that FTP, while showing strong affinity for AD-type aggregates, still retains limited binding to early or non-AD tau aggregates, including in non-AD tauopathies.[41–43]

The close correlation between EEG features such as slowing and multifocal discharges and regional FTP SUVRs suggests an association between pervasive neuronal network dysfunction and increased FTP uptake. This finding also aligns with emerging evidence that tau can be dynamically modulated, with hyperexcitability promoting tau release and spread.[44,45] Recurrent epileptiform discharges and low frequency slowing on EEG could in turn also be markers of a permissive environment for pathological tau accumulation.

In our study, we observed globally increased FTP SUVRs across all brain regions in every type of epilepsy examined, even in focal epilepsy cases with likely localised seizure onset zones. Simultaneously, asymmetry of putative tau accumulation suggested a bias towards the epileptogenic hemisphere, especially in the lateral cortical regions, concordant with a bias in EEG to better detect localise seizure onset zones in lateral cortical regions. Moreover, patients with hippocampal sclerosis had elevated average tau tracer uptake in the medial temporal cortex outside of the atrophic hippocampus. These findings suggest that while epilepsy may exert widespread effects resulting in elevated tau deposition throughout the brain, localised tau accumulation may occur preferentially in the abnormal cortical area.

Interestingly, elevation of FTP SUVR was most pronounced in patients with postencephalitic epilepsy, alluding to inflammatory etiologies in the pathogenesis of tau accumulation. This is supported by our proteomic analysis, which revealed that proteins positively associated with regional FTP tracer signal were enriched in pathways involved in the immune system, with

innate components such as TCR signalling, cytokine signalling, IL-17, and leukocyte chemotaxis implicated. Enriched pathways in common from the set of overexpressed proteins in epilepsy and proteins positively correlated with regional FTP SUVRs included ErbB signalling, which is a key regulator of inflammation.

Focus on individual proteins in the proteomic analyses further suggested several candidate molecular pathways underlying epilepsy-associated tau accumulation. Epilepsy patients exhibited increased peripheral presence of proteins involved in cellular maintenance, proteostasis, and protein quality control. Epilepsy was also accompanied by reduced abundance of proteins related to energy metabolism and structural integrity. Our findings align with previous studies reporting increased ribosomal proteins and decreased mitochondrial respirasome proteins in the hippocampi epilepsy patients.[17,46] In turn, proteins nominally associated with regional FTP uptake included proteins associated with metabolic adaptation and oxidative stress defense, aligning with and growing evidence linking mitochondrial dysfunction to tau deposition and neurodegenerative disease progression.[47–49] Proteins involved in microglial activation, immune cell recruitment, and immunomodulation were associated with decreased regional FTP uptake, hinting at immune mechanisms playing an important role in the clearance of tau.

Beyond molecular pathways, we observed that organ age gaps, particularly in the brain, heart, and muscle, showed a trend toward positive association with regional FTP uptake. Associations between organ age gaps and regional FTP SUVRs were in general more positive in the control group, indicating that tau in controls better reflect systemic ageing related changes. However, brain, heart, and muscle age gaps had positive correlations in the epilepsy group. Organ age gaps also correlated with epilepsy-related clinical factors, indicating a more complex, yet unexplored interrelationship between organ ageing, brain FTP uptake, and clinical severity. Organ age gap may capture a combination of epilepsy-related changes and nonspecific ageing, and our findings should be interpreted within the constraints of cross-sectional inference, and future studies with longitudinal data are required to investigate this hypothesis further.

To minimise confounding from dementia-spectrum pathology in older adults and from developmental or non–epilepsy–related factors in younger individuals, we restricted enrollment to patients without subjective memory complaints. Our aim was to evaluate whether tau accumulation occurs as part of a process intrinsic to epilepsy, rather than reflecting co-occurring

neurodegenerative or neurodevelopmental conditions. Nevertheless, one limitation of our study is that our findings may not fully generalise to all individuals with epilepsy, particularly those with overt cognitive impairment.

Several important caveats must be mentioned in the interpretation of our PET findings. Although the 80–100-minute acquisition window substantially minimises flow-related variability in FTP SUVR[50,51] and cerebellar involvement as a reference region for SUVR was unlikely in our cohort given the absence abnormal cerebellar perfusion in perfusion imaging performed for a subset of patients (**Supplementary Table 12)**, it must be acknowledged that the possibility of altered tracer delivery or wash-out due to regional perfusion abnormalities in epilepsy cannot be excluded. Integrating blood flow measures in future studies would further clarify the relationship between perfusion and tau-associated tracer retention in epilepsy.[51,52]

It is also crucial to note that FTP was originally developed to target AD paired helical filament (PHF) tau and that it binds less well to other conformations of tau. The tau deposits observed in surgical specimen and postmortem tissue of epilepsy patients include both 3-repeat and 4-repeat tau, as in AD, but exist in a more fragmented or oligomeric form rather than fully assembled PHF.[10,11,53] Moreover, FTP exhibits known off-target uptake in regions such as the basal ganglia, choroid plexus, meninges, and monoamine-oxidase-B (MAO-B) rich structures (**Supplementary Figure 25**), which could contribute to apparent cortical signal increases independent of tau aggregation.[51] We excluded the basal ganglia from the analysis for this reason and conducted a separate analysis after excluding the hippocampus from the medial temporal lobe, where elevated average FTP SUVR was still evident, consistent with previous reports of tau in epileptic regions.[53-55] MAO-B is upregulated in reactive astrocytes,[56] and reactive astrogliosis is common pathological feature in chronic epilepsy.[57,58] Accordingly, a portion of the increased FTP uptake may be attributable to reactive gliosis rather than primary tauopathy. Nevertheless, this does not preclude its potential utility as a biomarker, as the tracer signal may still capture clinically meaningful pathological processes associated with disease burden and chronicity. A further limitation of our study is that we did not implement a voxel-wise partial volume correction. Consequently, the reported signal intensities may be subject to partial volume effects, particularly in regions adjacent to CSF spaces or in atrophic brain regions.

Other limitations of our study include the small sample size, limiting statistical power and generalizability; the lack of extensive cognitive evaluation in the epilepsy patients and controls; and the lack of precise anatomical seizure onset zone localization that could have indicated whether greater tau accumulation occurred within the seizure onset zones. Prior literature has repeatedly demonstrated an association between excessive tau deposition and cognitive and memory dysfunction in epilepsy patients.[11–13] While our patients did not have memory complaints and had normal MMSE scores, they may have demonstrated deficits in detailed cognitive testing. Future studies with larger, multicenter cohorts, detailed neurocognitive evaluation and high-resolution electrophysiological localization will be essential to validate and extend our findings and further elucidate the relationship between epilepsy and tau pathology.

In conclusion, our findings indicate that globally increased tau tracer signals are present even in patients without cognitive complaints in epilepsy, and may be associated with inflammatory etiologies, greater clinical severity, and accelerated systemic ageing. These results have potential implications for informing the development of biomarker-driven, disease-modifying interventions targeting tau-related mechanisms in epilepsy.

## Data availability

Data used in this study will be provided by the corresponding author upon reasonable request.

## Funding

This work was supported by the National Research Foundation of Korea (NRF) grant (NRF-2021R1A2C200846911) and Korea Medical Device Development Fund (the Ministry of Science and ICT, the Ministry of Trade, Industry and Energy, the Ministry of Health & Welfare, the Ministry of Food and Drug Safety) (Project Number: 1711137868, RS-2020-KD000006), both funded by the Korean government.

# Competing interests

The authors report no competing interests.

# Supplementary material

Supplementary material is available at *Brain* online.

# References


1. Weingarten MD, Lockwood AH, Hwo SY, Kirschner MW. A protein factor essential for microtubule assembly. Proceedings of the National Academy of Sciences. 1975;72(5):1858-1862. doi:10.1073/pnas.72.5.1858

2. Wang Y, Mandelkow E. Tau in physiology and pathology. Nat Rev Neurosci. 2016;17(1):22-35. doi:10.1038/nrn.2015.1

3. Arriagada PV, Growdon JH, Hedley-Whyte ET, Hyman BT. Neurofibrillary tangles but not senile plaques parallel duration and severity of Alzheimer's disease. Neurology. 1992;42(3):631-631. doi:10.1212/WNL.42.3.631

4. Yamada K, Cirrito JR, Stewart FR, et al. In Vivo Microdialysis Reveals Age-Dependent Decrease of Brain Interstitial Fluid Tau Levels in P301S Human Tau Transgenic Mice. J Neurosci. 2011;31(37):13110-13117. doi:10.1523/JNEUROSCI.2569-11.2011

5. Gomez-Murcia V, Sandau U, Ferry B, et al. Hyperexcitability and seizures in the THY-Tau22 mouse model of tauopathy. Neurobiology of Aging. 2020;94:265-270. doi:10.1016/j.neurobiolaging.2020.06.004

6. García-Cabrero AM, Guerrero-López R, Giráldez BG, et al. Hyperexcitability and epileptic seizures in a model of frontotemporal dementia. Neurobiology of Disease. 2013;58:200-208. doi:10.1016/j.nbd.2013.06.005

7. DeVos SL, Goncharoff DK, Chen G, et al. Antisense Reduction of Tau in Adult Mice Protects against Seizures. J Neurosci. 2013;33(31):12887-12897. doi:10.1523/JNEUROSCI.2107-13.2013

8. Gheyara AL, Ponnusamy R, Djukic B, et al. Tau reduction prevents disease in a mouse model of D ravet syndrome. Annals of Neurology. 2014;76(3):443-456. doi:10.1002/ana.24230

9. Holth JK, Bomben VC, Reed JG, et al. Tau Loss Attenuates Neuronal Network Hyperexcitability in Mouse and Drosophila Genetic Models of Epilepsy. J Neurosci. 2013;33(4):1651-1659. doi:10.1523/JNEUROSCI.3191-12.2013

10. Thom M, Liu JYW, Thompson P, et al. Neurofibrillary tangle pathology and Braak staging in chronic epilepsy in relation to traumatic brain injury and hippocampal sclerosis: a post-mortem study. Brain. 2011;134(10):2969-2981. doi:10.1093/brain/awr209

11. Toscano ECB, Vieira ÉLM, Grinberg LT, et al. Hyperphosphorylated Tau in Mesial Temporal Lobe Epilepsy: a Neuropathological and Cognitive Study. Mol Neurobiol. 2023;60(4):2174-2185. doi:10.1007/s12035-022-03190-x

12. Tai XY, Koepp M, Duncan JS, et al. Hyperphosphorylated tau in patients with refractory epilepsy correlates with cognitive decline: a study of temporal lobe resections. Brain. 2016;139(9):2441-2455. doi:10.1093/brain/aww187

13. Gourmaud S, Shou H, Irwin DJ, et al. Alzheimer-like amyloid and tau alterations associated with cognitive deficit in temporal lobe epilepsy. Brain. 2020;143(1):191-209. doi:10.1093/brain/awz381

14. Smith R, Schöll M, Leuzy A, et al. Head-to-head comparison of tau positron emission tomography tracers [18F]flortaucipir and [18F]RO948. Eur J Nucl Med Mol Imaging. 2020;47(2):342-354. doi:10.1007/s00259-019-04496-0

15. Marquié M, Normandin MD, Vanderburg CR, et al. Validating novel tau positron emission tomography tracer [F-18]-AV-1451 (T807) on postmortem brain tissue. Annals of Neurology. 2015;78(5):787-800. doi:10.1002/ana.24517

16. Gold L, Ayers D, Bertino J, et al. Aptamer-Based Multiplexed Proteomic Technology for Biomarker Discovery. PLOS ONE. 2010;5(12):e15004. doi:10.1371/journal.pone.0015004

17. Leitner D, Pires G, Kavanagh T, et al. Similar brain proteomic signatures in Alzheimer's disease and epilepsy. Acta Neuropathol. 2024;147(1):27. doi:10.1007/s00401-024-02683-4

18. Ma M, Cheng Y, Hou X, et al. Serum biomarkers in patients with drug-resistant epilepsy: a proteomics-based analysis. Front Neurol. 2024;15. doi:10.3389/fneur.2024.1383023

19. Hirsch LJ, Fong MWK, Leitinger M, et al. American Clinical Neurophysiology Society's Standardized Critical Care EEG Terminology: 2021 Version. Journal of Clinical Neurophysiology. 2021;38(1):1. doi:10.1097/WNP.0000000000000806

20. Kang SK, Kim D, Shin SA, Kim YK, Choi H, Lee JS. Fast and Accurate Amyloid Brain PET Quantification Without MRI Using Deep Neural Networks. Journal of Nuclear Medicine. 2023;64(4):659-666. doi:10.2967/jnumed.122.264414

21. Sabri O, Seibyl J, Rowe C, Barthel H. Beta-amyloid imaging with florbetaben. Clin Transl Imaging. 2015;3(1):13-26. doi:10.1007/s40336-015-0102-6

22. Oh HSH, Rutledge J, Nachun D, et al. Organ aging signatures in the plasma proteome track health and disease. Nature. 2023;624(7990):164-172. doi:10.1038/s41586-023-06802-1

23. Ashton NJ, Brum WS, Di Molfetta G, et al. Diagnostic Accuracy of a Plasma Phosphorylated Tau 217 Immunoassay for Alzheimer Disease Pathology. JAMA Neurol. 2024;81(3):255-263. doi:10.1001/jamaneurol.2023.5319

24. Paul MS, Duncan AR, Genetti CA, et al. Rare EIF4A2 variants are associated with a neurodevelopmental disorder characterized by intellectual disability, hypotonia, and epilepsy. The American Journal of Human Genetics. 2023;110(1):120-145. doi:10.1016/j.ajhg.2022.11.011

25. Sapir T, Reiner O. HNRNPU's multi-tasking is essential for proper cortical development. BioEssays. 2023;45(9):2300039. doi:10.1002/bies.202300039

26. Tilliole P, Fix S, Godin JD. hnRNPs: roles in neurodevelopment and implication for brain disorders. Front Mol Neurosci. 2024;17. doi:10.3389/fnmol.2024.1411639

27. Soon HR, Gaunt JR, Bansal VA, Lenherr C, Sze SK, Ch'ng TH. Seizure enhances SUMOylation and zinc-finger transcriptional repression in neuronal nuclei. iScience. 2023;26(9). doi:10.1016/j.isci.2023.107707

28. Schorova L, Martin S. Sumoylation in Synaptic Function and Dysfunction. Front Synaptic Neurosci. 2016;8. doi:10.3389/fnsyn.2016.00009

29. Poliquin S, Kang JQ. Disruption of the Ubiquitin-Proteasome System and Elevated Endoplasmic Reticulum Stress in Epilepsy. Biomedicines. 2022;10(3):647. doi:10.3390/biomedicines10030647

30. Fu R, Fang L, Liu J, et al. Mitochondrial-associated endoplasmic reticulum membranes (MAMs) drive ferroptosis via redox signaling: A key potential mechanism in epilepsy. Neurobiology of Disease. Published online December 25, 2025:107248. doi:10.1016/j.nbd.2025.107248

31. Raza ML, Imam MH, Zehra W, Anwar IB, Mehdi R. Oxidative stress and neuronal alteration: Mitochondrial dysfunction as a key player in intractable epilepsy - a narrative

review. Pathology - Research and Practice. 2026;277:156285. doi:10.1016/j.prp.2025.156285

32. Yang X, Zhang J, Wang Z, et al. Mitochondria-related HSDL2 is a potential biomarker in temporal lobe epilepsy by modulating astrocytic lipid metabolism. Neurotherapeutics. 2024;21(6):e00447. doi:10.1016/j.neurot.2024.e00447

33. Tracy TE, Madero-Pérez J, Swaney DL, et al. Tau interactome maps synaptic and mitochondrial processes associated with neurodegeneration. Cell. 2022;185(4):712-728.e14. doi:10.1016/j.cell.2021.12.041

34. Zheng J, Akbari M, Schirmer C, et al. Hippocampal tau oligomerization early in tau pathology coincides with a transient alteration of mitochondrial homeostasis and DNA repair in a mouse model of tauopathy. Acta Neuropathologica Communications. 2020;8(1):25. doi:10.1186/s40478-020-00896-8

35. Lam AD, Thibault EG, Mayblyum DV, et al. Association of Seizure Foci and Location of Tau and Amyloid Deposition and Brain Atrophy in Patients With Alzheimer Disease and Seizures. Neurology. 2024;103(9):e209920. doi:10.1212/WNL.0000000000209920

36. Joutsa J, Rinne JO, Niemi KJ, et al. Progression of Amyloid Accumulation in Late Adulthood Among People With Childhood-Onset Epilepsy. Neurology. 2025;104(3):e210303. doi:10.1212/WNL.0000000000210303

37. Josephs KA, Tosakulwong N, Weigand SD, et al. Flortaucipir PET uncovers relationships between tau and amyloid-β in primary age–related tauopathy and Alzheimer's disease. Science Translational Medicine. Published online 2024.

38. Chen SD, Lu JY, Li HQ, et al. Staging tau pathology with tau PET in Alzheimer's disease: a longitudinal study. Transl Psychiatry. 2021;11(1):1-12. doi:10.1038/s41398-021-01602-5

39. Ising C, Venegas C, Zhang S, et al. NLRP3 inflammasome activation drives tau pathology. Nature. 2019;575(7784):669-673. doi:10.1038/s41586-019-1769-z

40. Langworth-Green C, Patel S, Jaunmuktane Z, et al. Chronic effects of inflammation on tauopathies. The Lancet Neurology. 2023;22(5):430-442. doi:10.1016/S1474-4422(23)00038-8

41. Ossenkoppele R, Rabinovici GD, Smith R, et al. Discriminative Accuracy of [18F]flortaucipir Positron Emission Tomography for Alzheimer Disease vs Other Neurodegenerative Disorders. JAMA. 2018;320(11):1151-1162. doi:10.1001/jama.2018.12917

42. Cho H, Seo SW, Choi JY, et al. Predominant subcortical accumulation of 18F-flortaucipir binding in behavioral variant frontotemporal dementia. Neurobiology of Aging. 2018;66:112-121. doi:10.1016/j.neurobiolaging.2018.02.015

43. Groot C, Villeneuve S, Smith R, Hansson O, Ossenkoppele R. Tau PET Imaging in Neurodegenerative Disorders. Journal of Nuclear Medicine. 2022;63(Supplement 1):20S-26S. doi:10.2967/jnumed.121.263196

44. Devulder A, Vanderlinden G, Van Langenhoven L, et al. Epileptic activity on foramen ovale electrodes is associated with sleep and tau pathology in Alzheimer's disease. Brain. 2025;148(2):506-520. doi:10.1093/brain/awae231

45. Perellón-Alfonso R, Abellaneda-Pérez K, Pileckyte I, et al. Spontaneous and perturbation-based EEG cortical excitability markers are associated with plasma p-tau181 concentration in healthy middle-aged adults. Heliyon. 2024;10(24):e41118. doi:10.1016/j.heliyon.2024.e41118

46. Pires G, Leitner D, Drummond E, et al. Proteomic differences in the hippocampus and cortex of epilepsy brain tissue. Brain Communications. 2021;3(2):fcab021. doi:10.1093/braincomms/fcab021

47. Terada T, Therriault J, Kang MSP, et al. Mitochondrial complex I abnormalities is associated with tau and clinical symptoms in mild Alzheimer's disease. Mol Neurodegeneration. 2021;16(1):28. doi:10.1186/s13024-021-00448-1

48. Du F, Yu Q, Swerdlow RH, Waites CL. Glucocorticoid-driven mitochondrial damage stimulates Tau pathology. Brain. 2023;146(10):4378-4394. doi:10.1093/brain/awad127

49. Kemna RE, Kueck PJ, Honea R, et al. Mitochondrial DNA affects tau phosphorylation in aging and Alzheimer's disease. Alzheimer's & Dementia. 2025;21(7):e70390. doi:10.1002/alz.70390

50. Tian M, Civelek AC, Carrio I, et al. International consensus on the use of tau PET imaging agent 18F-flortaucipir in Alzheimer's disease. Eur J Nucl Med Mol Imaging. 2022;49(3):895-904. doi:10.1007/s00259-021-05673-w

51. Baker SL, Harrison TM, Maaß A, Joie RL, Jagust W. Effect of off-target binding on 18F-Flortaucipir variability in healthy controls across the lifespan. Journal of Nuclear Medicine. Published online March 1, 2019. doi:10.2967/jnumed.118.224113

52. Shcherbinin S, Schwarz AJ, Joshi A, et al. Kinetics of the Tau PET Tracer 18F-AV-1451 (T807) in Subjects with Normal Cognitive Function, Mild Cognitive Impairment, and

Alzheimer Disease. Journal of Nuclear Medicine. 2016;57(10):1535-1542. doi:10.2967/jnumed.115.170027

53. Sen A, Thom M, Martinian L, et al. Pathological Tau Tangles Localize to Focal Cortical Dysplasia in Older Patients. Epilepsia. 2007;48(8):1447-1454. doi:10.1111/j.1528-1167.2007.01107.x

54. Aroor A, Nguyen P, Li Y, Das R, Lugo JN, Brewster AL. Assessment of tau phosphorylation and β-amyloid pathology in human drug-resistant epilepsy. Epilepsia Open. 2023;8(2):609-622. doi:10.1002/epi4.12744

55. Alves M, Kenny A, de Leo G, Beamer EH, Engel T. Tau Phosphorylation in a Mouse Model of Temporal Lobe Epilepsy. Front Aging Neurosci. 2019;11. doi:10.3389/fnagi.2019.00308

56. Jaisa-aad M, Muñoz-Castro C, Healey MA, Hyman BT, Serrano-Pozo A. Characterization of monoamine oxidase-B (MAO-B) as a biomarker of reactive astrogliosis in Alzheimer's disease and related dementias. Acta Neuropathol. 2024;147(1):66. doi:10.1007/s00401-024-02712-2

57. Johnson AM, Sugo E, Barreto D, et al. The Severity of Gliosis in Hippocampal Sclerosis Correlates with Pre-Operative Seizure Burden and Outcome After Temporal Lobectomy. Mol Neurobiol. 2016;53(8):5446-5456. doi:10.1007/s12035-015-9465-y

58. Egilmez A, Yen SF, Pauletti A, Bröer S. Reactive astrogliosis and microgliosis in animal models of focally induced seizures: A systematic review and multivariate multilevel meta-analysis. Epilepsy & Behavior. 2025;172:110694. doi:10.1016/j.yebeh.2025.110694

# Figure legends

**Figure 1 Regional [$^{18}$F]flortaucipir SUVR profiles and association with clinical factors in epilepsy and controls. (A)** Group-average [$^{18}$F]flortaucipir SUVR maps for epilepsy patients and controls projected onto brain slices. First and second rows display average tau SUVRs. The third row displays raw $-\log_{10} p$-values from sublobar region-based comparisons between groups. Brain slices are displayed from left to right. **(B)** Boxplots of regional tau SUVRs in cortical areas, comparing epilepsy patients (orange) and controls (green). *p*-values are from age- and sex- corrected linear models and FDR-adjusted. $^{*}$ FDR adjusted *p*-value < 0.05, $^{**}$ FDR adjusted *p*-value <0.01, $^{***}$ FDR adjusted *p*-value <0.005. Each datapoint represents the mean of left and right hemispheres. **(C-D)** Associations between clinical and EEG features and regional tau PET uptake: Heatmaps display partial

correlation coefficients (partial *r*) between EEG features and clinical history and regional FTP SUVRs across cortical regions. **(C)** left hemisphere, **(D)** right hemisphere. Partial correlation coefficients were calculated using partial correlation analyses adjusted for age and sex for continuous variables, and covariate-adjusted linear models for categorical variables. Asterisks denote nominal statistical significance (unadjusted *p*-value<0.05). Associations are shown for exploratory visualisation.

**Figure 2 Boxplots of regional [$^{18}$F]flortaucipir SUVR stratified by highlighted EEG and clinical features.** Boxplots show regional FTP SUVRs across cortical regions stratified by the presence (Yes) or absence (No) of multifocal interictal discharges **(A)**, EEG slowing **(B)**, and persistent seizures during adolescence **(C)**. Each box represents the median and interquartile range, with whiskers indicating 1.5× the interquartile range and individual data points representing the mean SUVR of left and right hemispheres overlaid. Grey line denotes SUVR = 1. Each dot represents the mean of left and right hemispheres. * FDR adjusted *p*-value < 0.05; *p*-values are from posthoc analyses

**Figure 3 Regional [$^{18}$F]flortaucipir SUVRs in epilepsy patients stratified by etiology and and asymmetry index distribution in lateralised epilepsy. (A)** Boxplots of regional tau SUVRs stratified by epilepsy etiology: generalised epilepsy (green), hippocampal sclerosis (salmon), nonlesional epilepsy (lavender), and postencephalitic epilepsy (pink). Postencephalitic epilepsy was associated with the highest overall tau burden. **(B)** Boxplots of asymmetry indices in patients with left-lateralised (blue) and right-lateralised (yellow) epilepsy. Green lines indicate mean asymmetry values of control subjects and shaded areas represent the standard error of the mean. The asymmetry index reflects the difference in SUVRs between hemispheres, with positive values indicating greater tau deposition in the left hemisphere. The most pronounced asymmetry differences between left and right lateralised epilepsy were observed in the lateral parietal, temporal, and occipital cortices.

**Figure 4 Individual-level distribution of [$^{18}$F]flortaucipir SUVR and cortical volume *Z* scores in representative cases.** Regional FTP SUVR *Z* score (left column) and cortical volume *Z* score distribution patterns for representative individual subjects displayed on standard brain maps. Warmer colors indicate higher-than-expected FTP uptake and colder colors indicate greater-than-expected atrophy. Maps are shown in multiple standard views with left (L) and right (R) hemispheres indicated. The right column summarises key clinical

and EEG characteristics for each individual. The middle sagittal slices for FTP and volume *Z* scores represent the medial surface of the right hemisphere. **(A)**, **(B)** Right and left-lateralised epilepsy patients with heterogeneous distribution of FTP uptake. **(C)** Patient with right hippocampal sclerosis. **(D)** Post-encephalitic epilepsy patient. **(E)** Unexpectedly high FTP SUVR and volume atrophy in a patient with drug-sensitive epilepsy, subsequently diagnosed with AD. AI: asymmetry index, SOZ: seizure onset zone, IED: interictal epileptiform discharges, ASM: antiseizure medication, Dur: epilepsy duration, T: temporal, F: frontal, P: parietal. *AIs for left-lateralised epilepsy are displayed as (L-R/L+R) and for right lateralised epilepsy as (R-L/R+L), and sagittal slices are displayed for the hemisphere of lateralisation. Warmer colors represent increased FTP SUVR in the hemisphere ipsilateral to the seizure onset zone compared to the contralateral hemisphere.

**Figure 5 Differentially expressed proteins between epilepsy and controls. (A)** Volcano plot of differential protein expression between epilepsy patients and controls. **(B)** Pathway enrichment analysis of overexpressed proteins using gProfiler, with gene ontology (GO), KEGG, WikiPathways, and Reactome databases. *p*-values from g:SCS (Set Counts and Sizes) correction.

**Figure 6 Pathway analysis of positively and negatively correlated proteins associated with brain regional tau deposition in epilepsy.** (A) Pathway enrichment analysis of 70 positively correlated proteins using Enrichr, with gene ontology (GO), KEGG, WikiPathways, and Reactome databases. *p*-values from g:SCS (Set Counts and Sizes) correction. (B) Pathway enrichment analysis of 54 negatively correlated proteins using Enrichr, with gene ontology (GO), KEGG, WikiPathways, and Reactome databases. *p*-values from g:SCS (Set Counts and Sizes) correction.

**Figure 7 Organ age gap differences between controls and epilepsy.** Boxplot of organ age gap *Z*-scores in controls (orange) and epilepsy (blue) across 11 organs and and conventional organ age. *P*-values are derived from sex-corrected comparison between epilepsy and controls. * unadjusted $p$-value < 0.05, ** unadjusted $p$-value <0.01, *** unadjusted $p$-value <0.005.

**Table 1 Demographic and Clinical Characteristics**

| Characteristic | Epilepsy (*N* = 75) | | Control (*N* = 47) | | *P*-value |
|---|---|---|---|---|---|
| | Epilepsy with Tau I (*N* = 32) | Epilepsy with P (*N* = 73) | Control with Tau I (*N* = 24) | Control with P (*N*=43) | |
| Age, mean (SD), years | 46.9 (19.1) | 41.8 (17.0) | 51.9 (15.4) | 48.9 (15.2) | 0.236[a] / 0.022[b,*] |
| Sex, female *n* (%) | 16 (50.0%) | 39 (53.4%) | 11 (45.8%) | 34 (46.5%) | 0.793[a] / 0.598[b] |
| APOE allele, *n* (%) | *n* = 40 | | *n* = 25 | | 0.568 |
| e2/e3 | 3 (7.5%) | | 2 (8.0%) | | – |
| e3/e3 | 28 (70.0%) | | 20 (80.0%) | | – |
| e3/e4 | 9 (22.5%) | | 3 (12.0%) | | – |
| BAPL | *n* = 20 | – | *n* = 7 | – | 0.610 |
| 1 | 18 (90.0%) | – | 6 (85.7%) | – | – |
| 2 | 1 (5.0%) | – | 0 (0.0%) | – | – |
| 3 | 1 (5.0%) | – | 1 (14.3%) | – | – |
| MMSE | 27.0 (3.0) | | 28.8 (1.8) | | 0.152 |
| PSQI | 8.8 (4.8) | | 11.0 (7.5) | | 0.709 |
| PHQ-9 | 14.4 (5.3) | | 12.4 (7.1) | | 0.246 |
| p-tau 217 | 0.44 (0.64) | 0.39 (0.56) | 0.26 (0.11) | 0.28 (0.23) | 0.166[a] / 0.272[b] |
| Total Tau | 3.35 (1.24) | 3.35 (1.21) | 3.41 (0.78) | 3.50 (0.84) | 0.885[a] / 0.660[b] |
| Amyloid-$\beta_{40/42}$ | 0.048 (0.01) | 0.047 (0.01) | 0.043 (0.01) | 0.046 (0.01) | 0.312[a] / 0.709[b] |
| **Epilepsy characteristics** | | | | | |
| Laterality | | | | | |
| Generalized | 3 (9.4%) | 3 (4.1%) | – | – | – |
| Left | 14 (43.8%) | 37 (50.6%) | – | – | – |
| Right | 9 (28.1%) | 25 (34.2%) | – | – | – |
| Bilateral | 5 (15.6%) | 5 (6.8%) | – | – | – |
| Unclear | 1 (3.1%) | 3 (4.1%) | – | – | – |
| Aetiology | | | | | |
| Idiopathic | 2 (6.2%) | 2 (2.7%) | – | – | – |
| HS | 3 (9.4%) | 11 (15.0%) | – | – | – |
| Non-lesional | 23 (71.8%) | 37 (50.7%) | – | – | – |
| Postencephalitic | 4 (12.5%) | 5 (6.8%) | – | – | – |
| Lesional | 0 (0%) | 18 (24.7%) | – | – | – |
| Number of ASM | | | | | |
| 1 | 10 (31.2%) | 32 (43.8%) | – | – | – |
| 2 | 10 (31.2%) | 13 (17.8%) | – | – | – |
| 3 | 5 (15.6%) | 15 (20.5%) | – | – | – |
| 4 or more | 7 (21.9%) | 13 (17.8%) | – | – | – |
| Seizure frequency (per month) | | | | | |
| 1 or less | 21 (65.6%) | 36 (49.3%) | – | – | – |
| 2 to 4 | 6 (18.8%) | 17 (23.2%) | – | – | – |
| More than 4 | 5 (15.6%) | 20 (27.4%) | – | – | – |
| Epilepsy duration (years) | | | | | |
| 1 y or less | 11 (34.4%) | 21 (28.8%) | – | – | – |
| 2 to 4 y | 8 (25.0%) | 16 (21.9%) | – | – | – |
| 5 to 9 y | 2 (6.2%) | 4 (5.5%) | – | – | – |
| 10 y or more | 11 (34.4%) | 32 (43.8%) | – | – | – |

Tau I = tau imaging with $^{18}$F-flortaucipir PET; P = proteomics with SOMAscan.

[a]*P*-value comparing Epilepsy with Tau I and Control with Tau I.

[b]*P*-value comparing Epilepsy with P and Control with P.

*P-value < 0.05

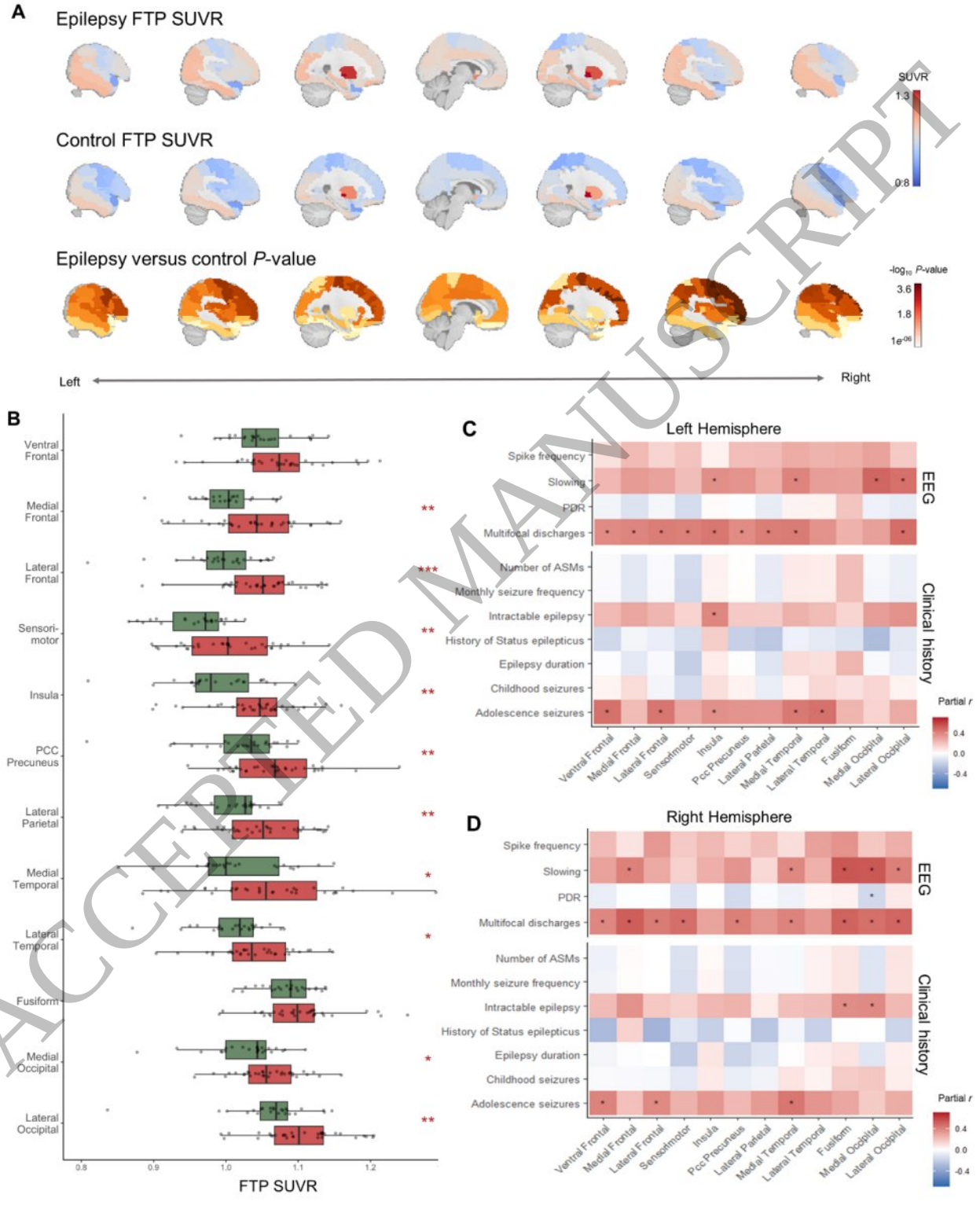


*Figure 1*
*165x204 mm (DPI)*

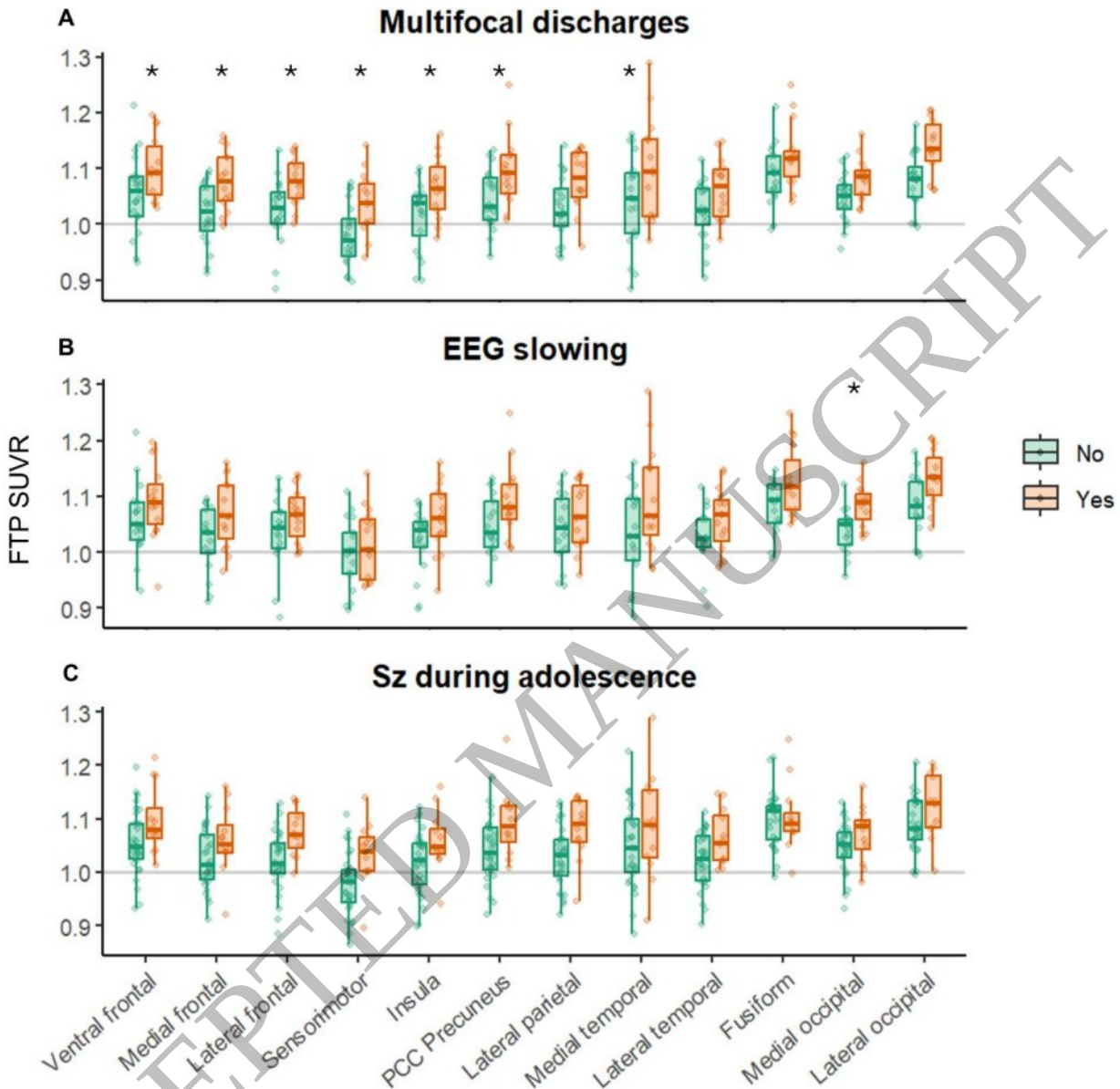


*Figure 2*
*165x162 mm (DPI)*

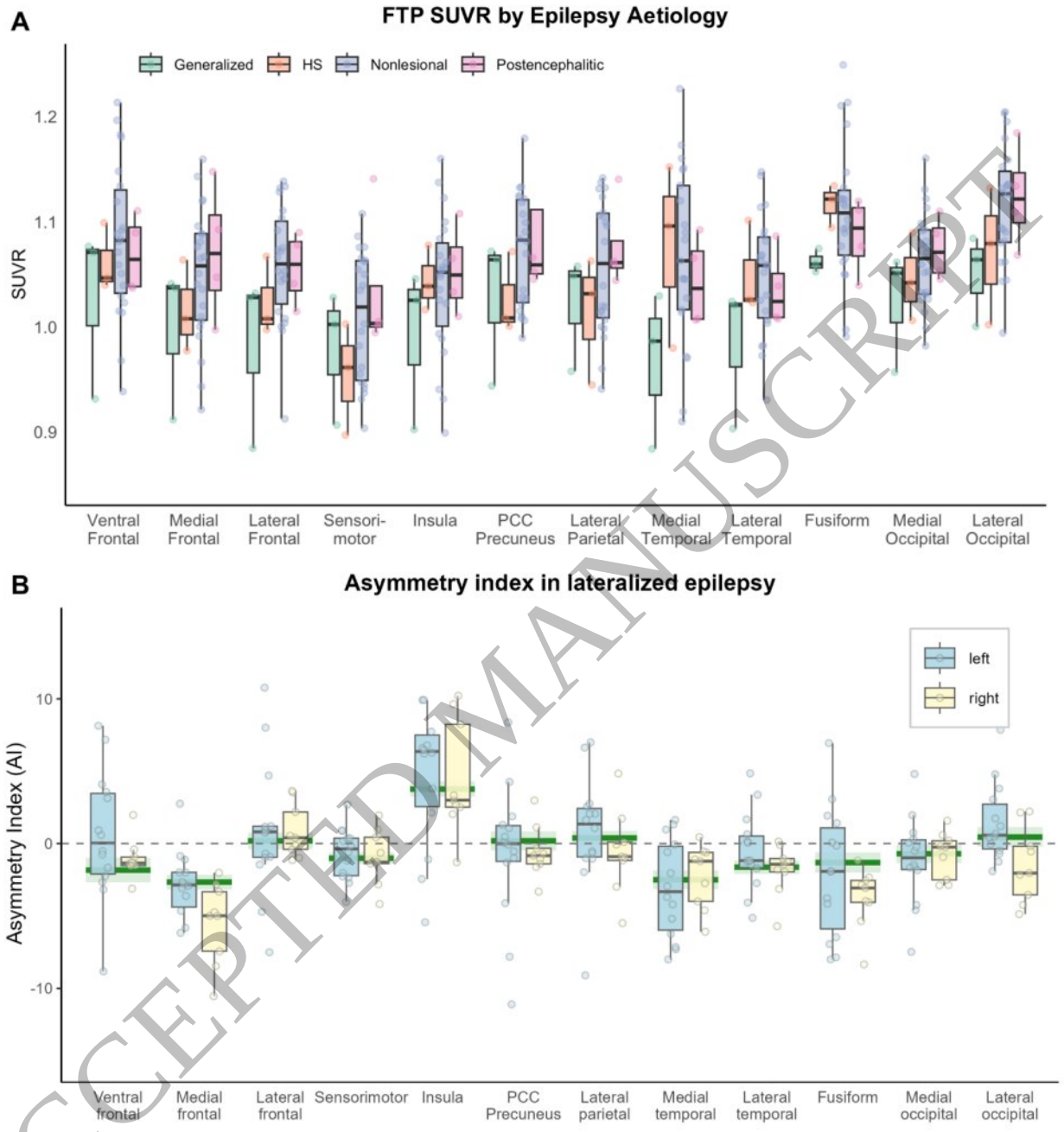


*Figure 3*
*165x176 mm (DPI)*

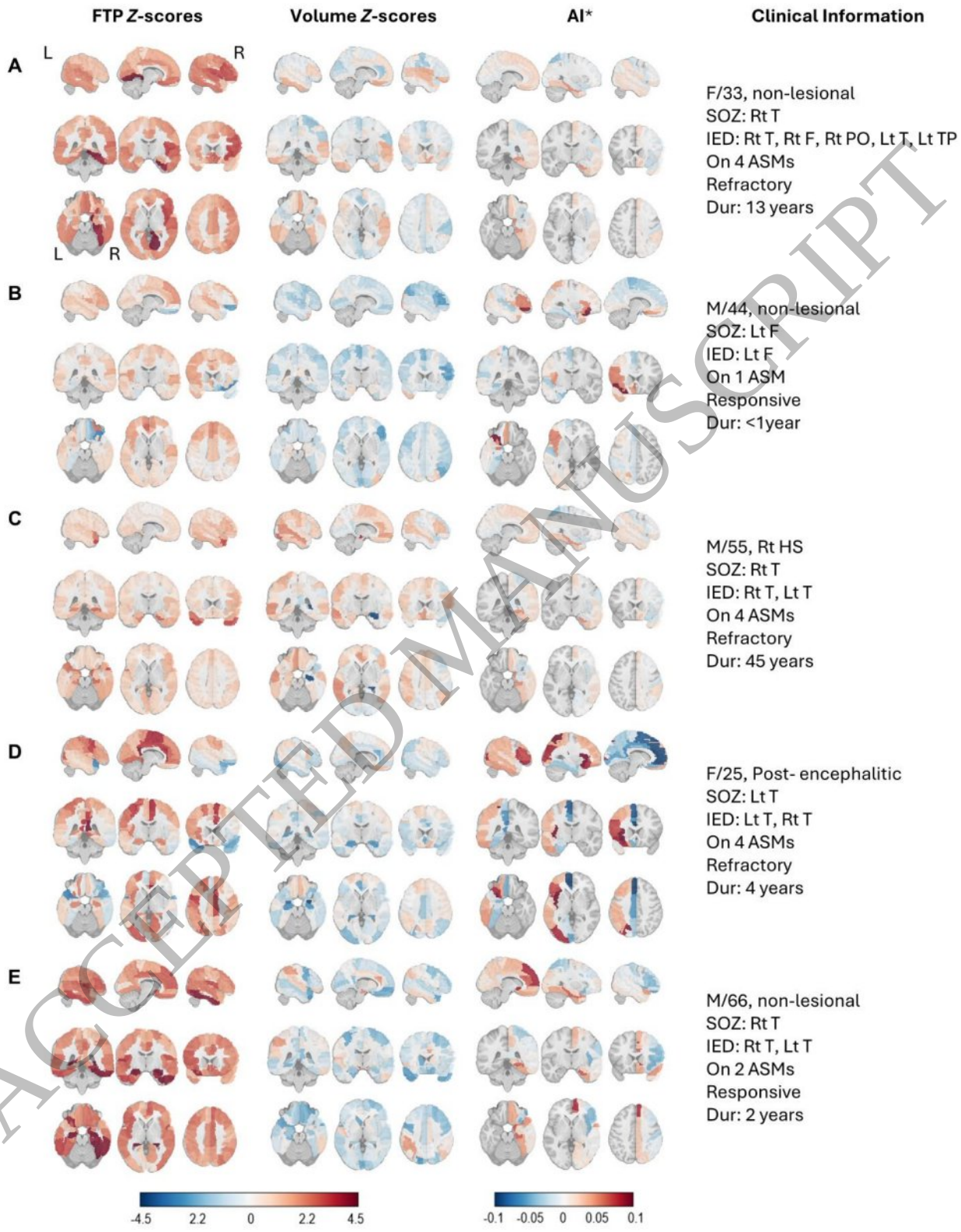


*Figure 4*
*165x211 mm (DPI)*

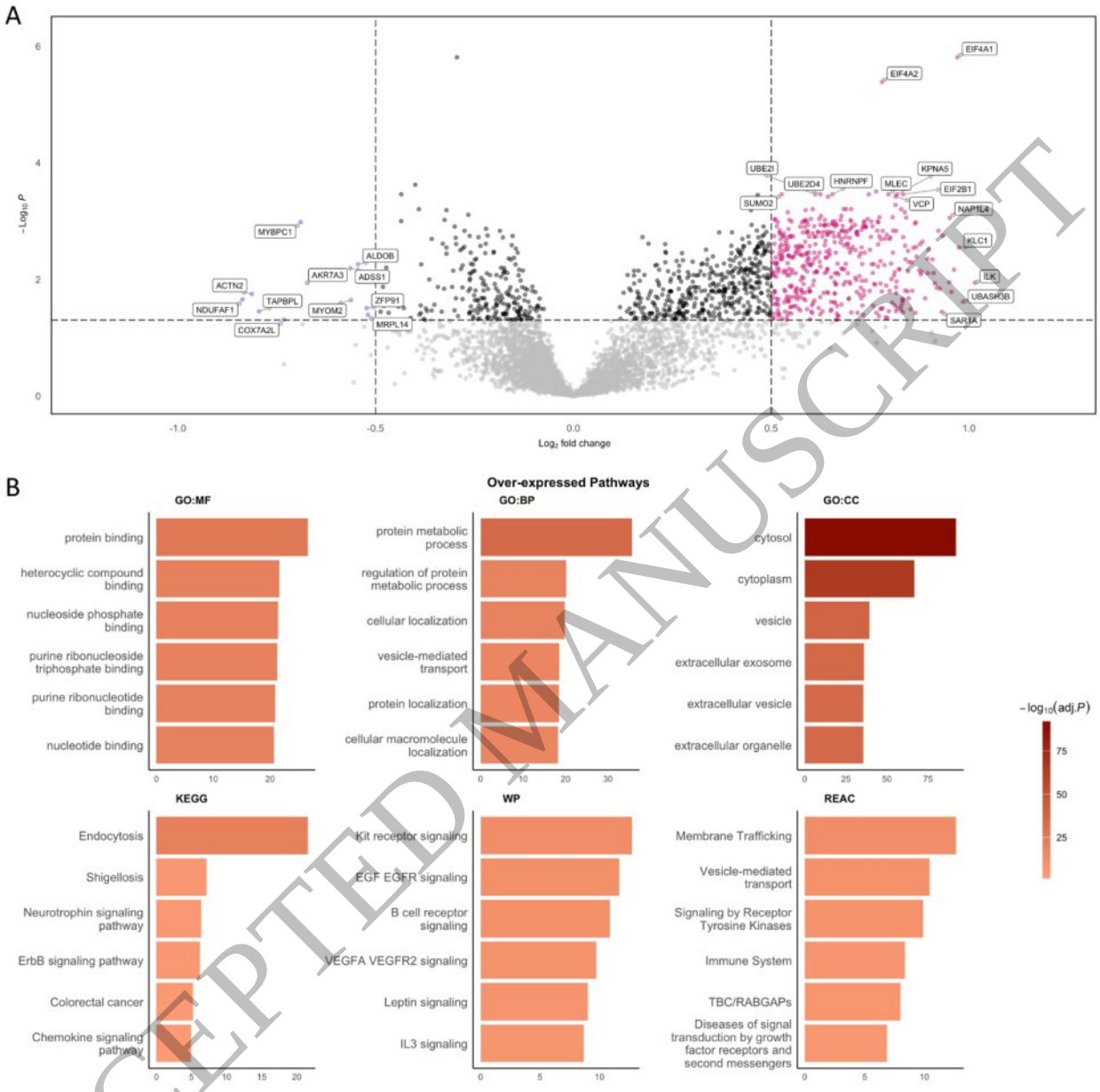


*Figure 5*
*165x166 mm (DPI)*

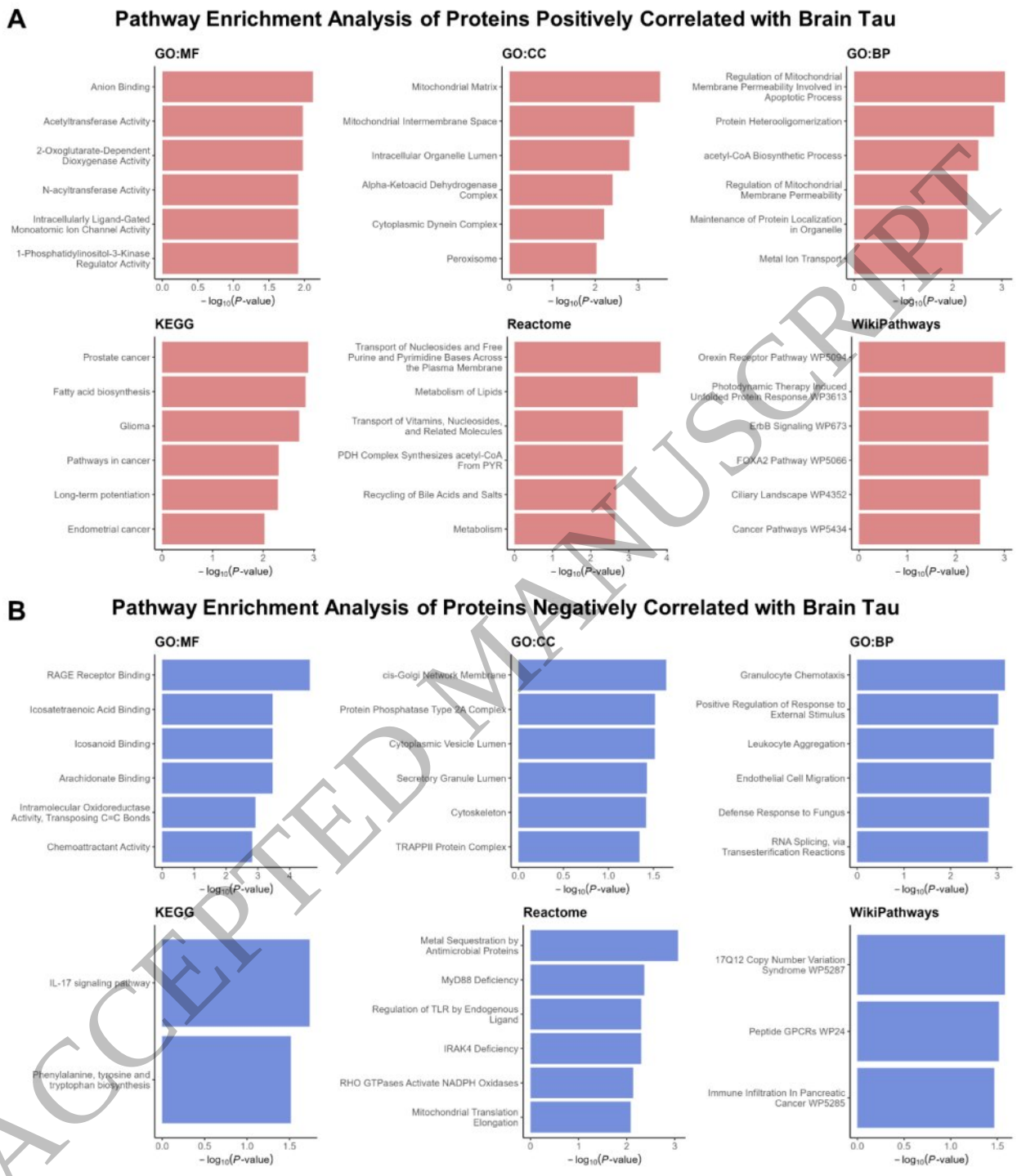


*Figure 6*
*165x192 mm (DPI)*

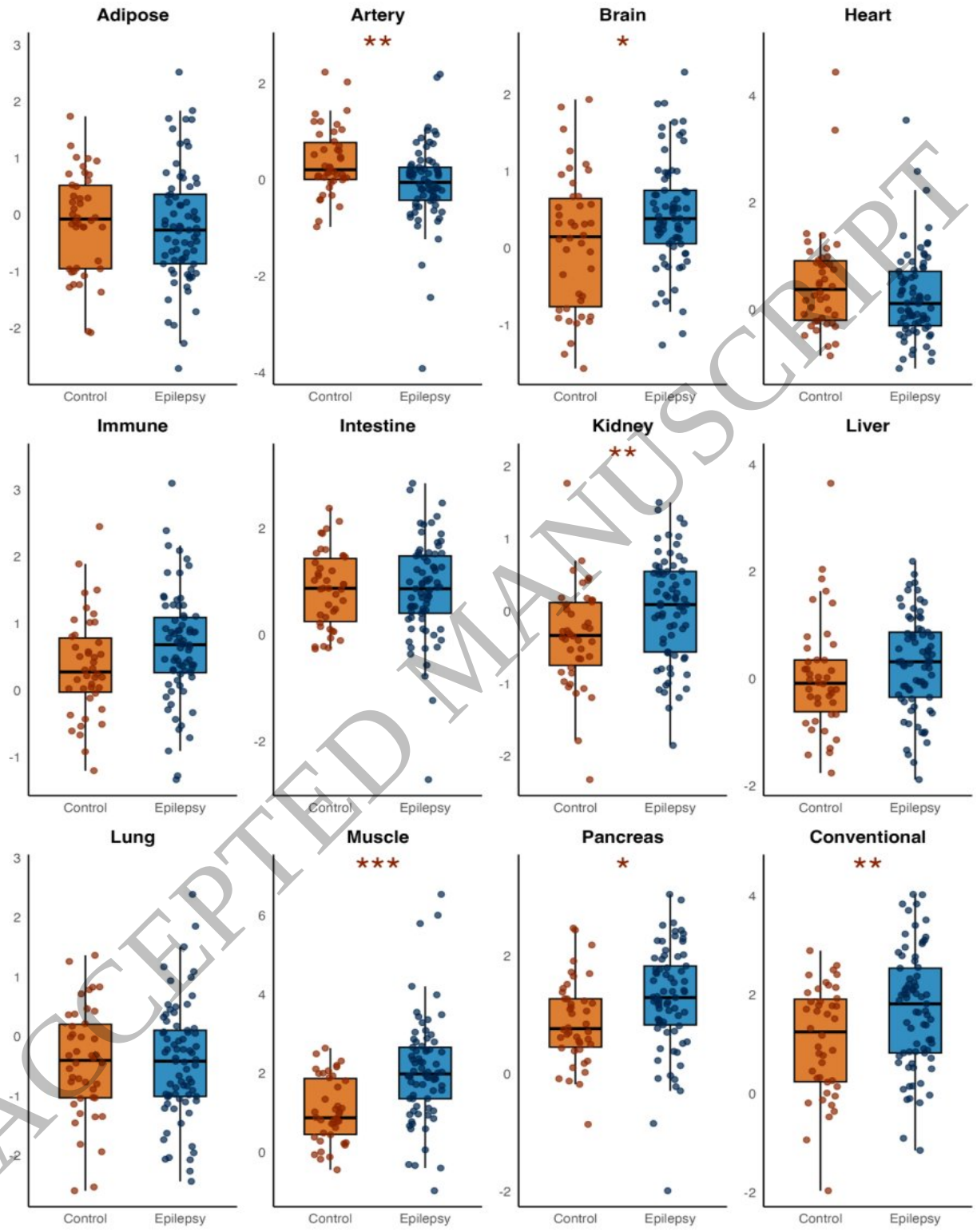


*Figure 7*
*165x219 mm (DPI)*